

## EVOLUTIONARY STRUCTURAL OPTIMIZATION BY EXTENSION TO COOL A FINITE-SIZE VOLUME GENERATING HEAT

G. Marck<sup>\*,1,2</sup>, M. Nemer<sup>1</sup>, D. Bougard<sup>2</sup>, S. Russeil<sup>2</sup>, J.-L. Harion<sup>2</sup>

<sup>1</sup> Paristech University, Center for Energy and Processes  
5, rue Léon Blum, F - 91120 Palaiseau - France

<sup>2</sup> Univ. Lille Nord de France, EMDouai  
764, boulevard Lahure, F - 59500 Douai - France

\*Correspondence author: Fax: +33 1 6919 4501 Email: gilles.marck@mines-paristech.fr

### ABSTRACT

The present study tackles the fundamental problem of cooling efficiently a finite-size volume generating heat with high conductivity material. The optimal organization of a finite amount of high conductivity material is still an open question and several different optimization methods put forward solutions leading to different designs. Ranging from constructal theory to morphing by gradient attraction, including metaheuristic methods, these approaches create tree-shaped cooling networks through the finite-size volume. The present work deals with an Evolutionary Structural Optimization (ESO) algorithm, which has been implemented in order to extend the cooling structure instead of degenerating its shape. Parallel calculation abilities have been developed allowing considering global objective functions such as the average temperature, instead of local temperature reductions. In addition to the valuable performances of the geometry reached, the history of construction provides further informations about the high conductivity layout. The results are compared with two geometries coming from constructal approach, under the same physical and geometrical assumptions.

### NOMENCLATURE

$A$  Adimensionalized average  
 $c$  Number of new candidate elements  
 $f$  Objective function

$\hat{k}$  Conductivity ratio ( $= k_p/k_0$ )  
 $m$  Element to test  
 $n_1$  Number of elemental volumes  
 $N$  Number of tested elements  
 $p$  Element to switch  
 $R$  Adimensionalized resistance  
 $\bar{T}$  Average temperature

### Greek letters

$\delta$  Boolean function of material  
 $\Phi$  Porosity ( $= V_{k_p}/(HL)$ )

### Subscripts

0 Elemental volume  
 1 First construct  
 $p$  High conductivity material  
 $s$  Heat sink

### INTRODUCTION

Among all the volume-to-point flow problems, one of the most addressed is linked with cooling operation. In [1], a fundamental problem is stated by Bejan as follows:

Consider a finite-size volume in which heat is being generated at every point, and which is cooled through a small patch (heat sink) located on its boundary. A finite amount of high conductivity ( $k_p$ ) material is available. Determine the optimal distribution of  $k_p$  material

through the given volume such that the highest temperature is minimized.

Several methods exist to create a high conductivity tree-network inside the finite-size volume, allowing draining heat to the sink. An example of construction method is constructal theory, which has been developed by Bejan in 1997 [1]: its philosophy lies on a process taking place from the smallest scales towards the largest ones. Its development has been partly based on the observation of organization in Nature and aims creating a bridge between physics and biology. However, in the frame of the problem tackled in this work, studies show that constructal theory is not optimal and too restrictive to be applied to real geometries [2, 3].

Another construction approach has been proposed by Xia *et al.* [4] in 2002, who titled it *bionic optimization*. It has been introduced in the frame of a two-dimensional heat conduction model involving a problem similar to [1] and has been followed by Cheng's work (*et al.*) [5]. The bionic principle considers the high conductivity material as being alive: its evolutionary principle involves that the growth is located where the maximum heat flux is. In 2009, Boichot *et al.* [6] used a similar method, named over *morphing by gradient attraction*, to rearrange  $k_p$  material from constructal geometries. They conclude their works underlining the unexplored field of cellular automaton applied to heat transfer.

Metaheuristic tools belong to the optimization processes widely applied to a large range of fields. Two specific metaheuristic schemes have been used to optimize the cooling structure made up of high conductivity material: simulated annealing (SA) and single-objective genetic algorithms (GAs). Xu *et al.* carried out SA and GAs implementations [7]: they made a comparison between the geometries coming from both metaheuristic approaches and other methods such as constructal theory or bionic optimization. In their conclusion, they point out the strong mesh dependency of their solutions.

Evolutionary Structural Optimization (ESO) is another way to shape design problems subjected to steady heat conduction. It has been borrowed to topology optimization in continuum and structural mechanics and Li *et al.* extended its methodology to heat conduction in 1999 [8, 9]. ESO principle lies on a discrete design variable method, also called 1 – 0 method. The

method is based on changing one of the main physical parameter of the elements constituting the mesh of a finite element or volume method. In the frame of heat conduction, ESO starts from a calculation field entirely made up of high conductivity material and removes it through a step-by-step approach based on a rejection ratio. The process stops when the optimization limits are reached, typically when the amount of  $k_p$  material becomes lower than the quantity wished.

The present work follows mainly the ESO philosophy such as it is defined in [8], constructing the cooling tree-network by arranging successively the high conductivity material. However, compared to [9], three differences are introduced allowing considering the problem from a more accurate angle thanks to a massive parallelization of the algorithmic scheme. At first, the sensitivity analysis is performed without making any assumption. Secondly, the traditional degenerative process has been reversed according to the nature of the problem: from now on, the high conductivity material is added to the cooling structure which starts its extension from the heat sink. Thirdly, the implemented objective functions are not restricted to temperature reductions in local points, but they can include global reduction such as average temperature.

First of all, the present study introduces the ESO algorithm by extension, pointing out the efforts made in code parallelization. Next, the influence of continuous  $k_p$  material extension is quantified in function of different objective functions. In completing, comparisons are made with results coming from constructal theory [1, 10]. Beyond quantitative aspects, the features of the cooling networks developed within this study possess similarities with the ones developed through the different enhancements of constructal approach [11–13].

## EVOLUTIONARY STRUCTURAL OPTIMIZATION BY EXTENSION

The physical parameters of the problem are described by Bejan in [1]. The energy differential equation driving the heat flux lies on several assumptions: at first, all the calculations are carried out under steady state conditions, meaning that the whole heat produced by the volume is evacuated through the heat sink. Secondly, material generating heat ( $k_0$ ) and high conductivity material ( $k_p$ ) are viewed as homogenous and isotropic, without effect of temperature on their respective con-

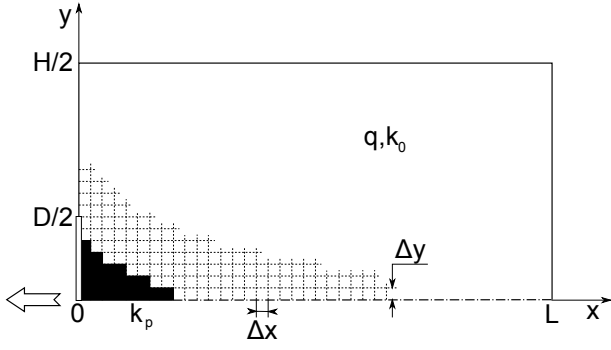


**FIGURE 1.** Physical and geometrical description of a rectangular finite-size volume including  $k_p$  material (in black) and  $k_0$  material (in white) with a structured mesh

ductivity. Throughout this study, it is also assumed that  $k_p$  material does not generate heat since it is added to the finite-size volume in order to cool it. Fig. 1 shows a classical geometry such as it is established for the calculation process.

**Problem introduction:** Defining  $q$  as the heat generation rate, the differential energy balance equation for the finite-size volume is :

$$\text{div}(k_i \mathbf{grad} T) + \delta_i q = 0 \quad \text{with} \quad \delta_i = \begin{cases} 0 & \text{if } i = p \quad (\text{high conductivity material}) \\ 1 & \text{if } i = 0 \quad (\text{material generating heat}) \end{cases} \quad (1)$$

The proof of Eq. 1 is widely available in literature, but [10] fully took it up in their work. In addition, three different boundary conditions are applied to the edges, as detailed in Fig. 1. At first, the hatched line pictures a symmetry condition along the x-axis: thanks to the geometry, calculations can only be run on the upper part, then reflected to the lower one. This condition is similar to the one describing the adiabatic edges, pictured with a black continuous line, and requires that the normal heat flux to each edge is equal to zero. The small black and white rectangle at the bottom left-hand corner pictures the heat sink location, which is characterized thanks to a Dirichlet boundary condition, namely  $T(0, y) = T_s$  for  $0 \leq y \leq D/2$ . Eq. 1 is solved thanks to finite volume method (FVM). The two-dimensional geometry is discretized into a finite number of control volumes, also shown in Fig. 1. The grid is cartesian and structured, which is perfectly suitable for regular geometry, and the thermal conductivity at cell interfaces is evaluated thanks to an harmonic mean.

**Setting up algorithm:** FVM allows evaluating the temperature field for all the possible  $k_p$  material configurations. The ESO algorithm rests on this numerical method to allocate high conductivity material, literally constructing the cooling network in a generative way. A sensitivity analysis must be led in order to identify the high conductivity elements to set up, namely the ones which will have a maximum impact on the objective function. The developed algorithm lies on the switch from  $k_0$  to  $k_p$  material of only one control volume per iteration step. An element has to fulfill two requirements to be switched: obviously, it must be made of  $k_0$  material, but it also has to be located on the boundary of the high conductivity structure being built. This second condition insures continuity through  $k_p$  material, whatever the shape of the cooling structure. Switching control volumes stops when a fraction  $\phi$  of the whole finite-size volume is reached, called porosity. The construction is performed thanks to two overlapped loops: the main one works on switching elements step by step to reach the wanted porosity, whereas the second one allows calculating the sensitivity of boundary elements (Fig. 2).

This second test loop aims scanning the set of  $k_0$  elements marking the boundary of  $k_p$  structure. However, since the calculation starts without high conductivity element, an initial boundary must be established to perform the first permutations. Two factors have oriented this initial choice: on one hand, the continuity assumption leads to connect every control volume made of  $k_p$  material to the heat sink. On the other hand, it stands to reason that an accumulation of high conductivity material is predictable around the heat sink as the whole generated heat goes through the region surrounding it. Consequently, the initial boundary shape is implemented along the heat sink, meaning that each control volume being next to it is a candidate for the first material permutation.

The sensitivity analysis along the  $k_p$  boundary is led by setting up each element with high-conductivity material and evaluating the objective function in this new configuration. The element which has the best impact on it is switched at the end of the main loop. This strategy leads to a significant problem concerning the calculation time. While a few control volumes are tested at the beginning of the ESO process, the time required by the sensitivity analysis is relatively short. Nonetheless, in conjunction with the structure rise, the number

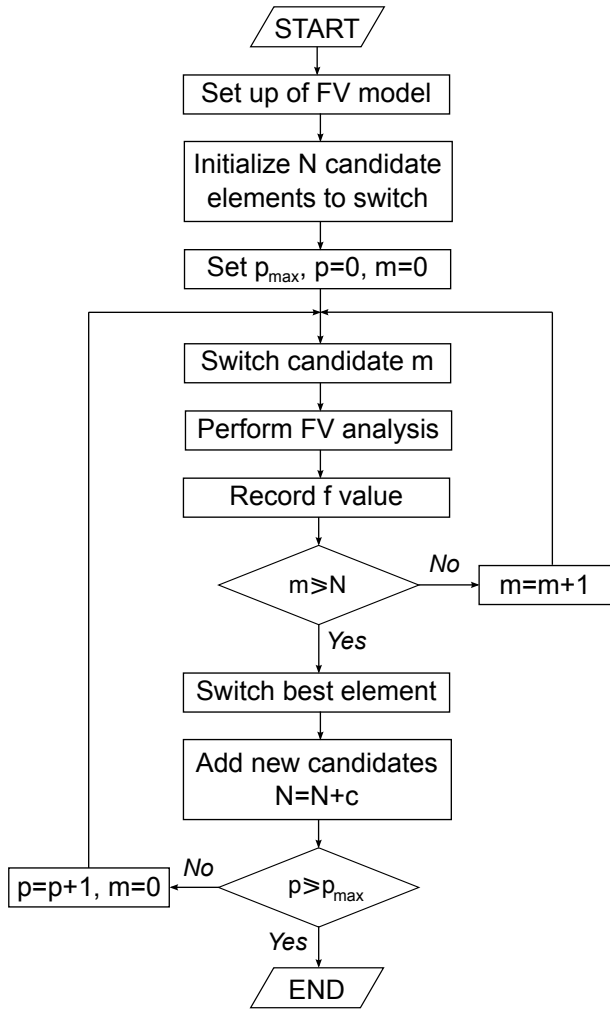


**FIGURE 2.** Specific ESO algorithm used in the present study

of tested elements becomes increasingly large, as well as the required calculation time. In order to resolve this specific problem, parallelization abilities have been developed, allowing calculating simultaneously different permutations. Concretely, the boundary is divided into the cores dedicated to the calculation. Fig. 3 details the parallelization for 4 cores (3 slaves and 1 master) and the determination of the best element.

The parallel test loops are performed independently by each slave, determining the best element to switch on their interval. Each best element is sent to the master process which collects all the best values of the objective function and only keeps the most efficient one. Once it has received the  $n^{th}$  value coming from the  $n^{th}$  slave, it broadcasts its switching decision to everyone before allowing the slaves starting their next test loops.

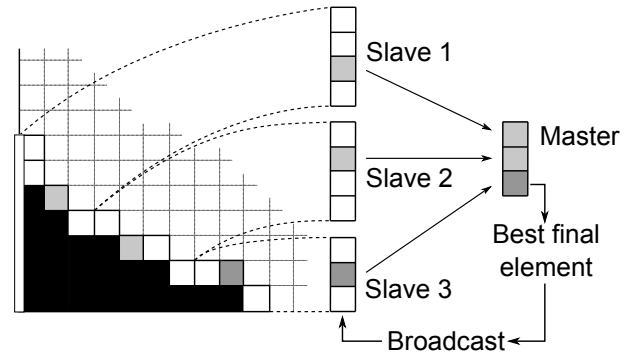


**FIGURE 3.** Operations of the parallel ESO algorithm on 4 cores (3 slaves and 1 master)

Obviously, the more the slaves are numerous, the more the calculation time is short. As so far, calculations have been run up to 80 slaves providing the results detailed in the next section.

The coupling between FVM and the evolutionary optimization methods is subject to some precautions regarding the independence of the final geometry to the mesh size. Different calculations have been run for the same external geometries with different sizes of cells: independence of the main structure is reached if the cell dimensions are below a critical a size, which has been set at  $2 \cdot 10^5$  cells/ $m^2$ . Even though this observation is correct for the skeleton of the  $k_p$  network, it is worth noting that the complexity of the thinnest structures is restricted by this critical value. All the results introduced in next section have been generated under this condition of mesh independence.

## RESULTS AND DISCUSSION

The results are interesting regarding two aspects: the shapes reached thanks to different objective functions and the history of construction. Calculations have been run with a square measuring 100 mm on each side, made of  $k_0$  material with a thermal conductivity of 1 W/ $m \cdot K$  and having a heat generation rate  $q = 10$  kW/ $m^3$ .  $k_p$  material has a conductivity of 500 W/ $m \cdot K$  with a maximal porosity of  $\phi = 20\%$ , and it is connected to a heat sink measuring 2 mm height. For each case after-specified, the grid size is strictly identical and made of 20000 square elements on half-size of the field ( $\Delta x = \Delta y = 0.5$ mm).

**Shape of cooling networks:** Two objective functions involving two opposite approaches have been investi-

gated: on one hand, a local temperature is reduced, and on the other hand, the global average temperature is minimized. These two criteria have been chosen to picture the differences inferred by a local or a global objective. The local optimization targets minimizing the temperature of the farthest point from the heat sink, namely the upper right-hand side corner:

$$\min f = T\left(L, \frac{H}{2}\right) - T(0,0) \quad (2)$$

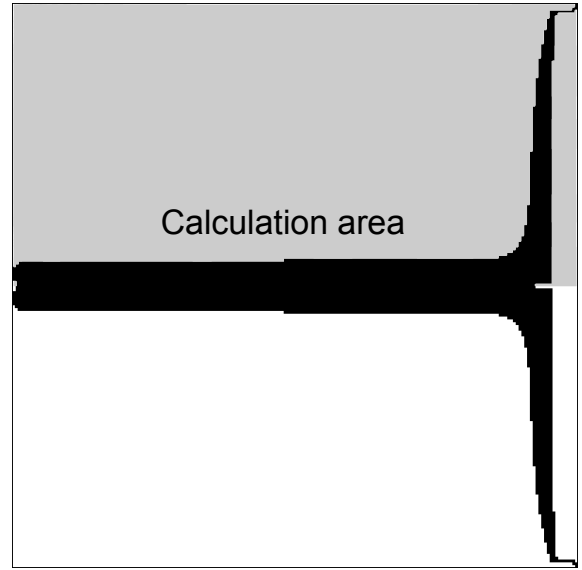
The other objective function tries to achieve a minimization of the temperature average, namely:

$$\min f = \frac{2}{HL} \int_0^L \int_0^{H/2} T(x,y) dx dy \quad (3)$$

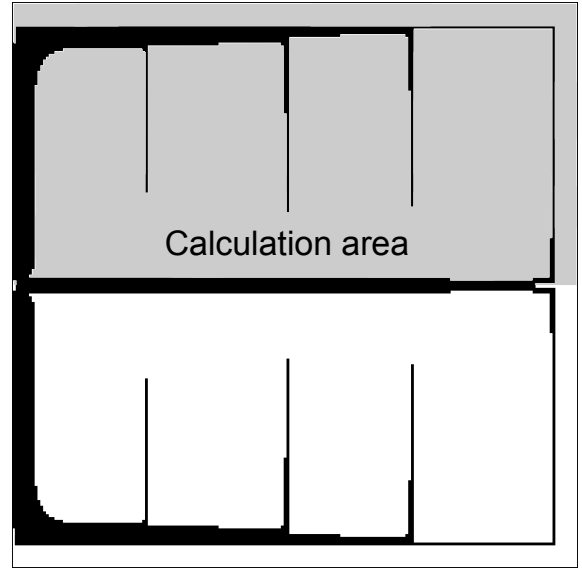
The reached geometries, shown on Fig. 4, have different shapes according of their objective function, as underlined in [9].  $k_p$  material added in order to reduce a local temperature is only dedicated to this task: the cooling network takes the shape of a link between the farthest corner and the heat sink, with a cross section becoming thinner through the finite-size volume. The main consequence of local objectives is that almost the whole field generating heat is left without any high conductivity material, since it only focuses on cooling a single control volume. The global objectives, such as average minimization, do not behave in the same way:  $k_p$  material is spread out through the finite-size volume with more spatial coherence. In some way, the cooling structure really tries connecting every control volume with the heat sink, leading to a tree-shaped network covering the whole area.

Through all the test cases run, the most interesting structures come from the temperature average reduction. These configurations have well-structured networks, especially if manufacturing constraints are taken into account. And secondly, the history of construction shows remarkable features which provide additional information about the way to construct the solution.

**History of construction:** Plotting the objective function values versus the porosity of the structure during the calculation process provides the history of solution construction. Coupling this plot with observations of shape modifications allows identifying key points during the construction steps. Fig. 5 shows these different



(a) Local temperature reduction



(b) Minimization of temperature average

**FIGURE 4.** Cooling network with a 2 mm heat sink and a porosity of  $\phi = 15\%$

states of the  $k_p$  material setting up for average objective. A parallel can be drawn between the scales of fractal theory and the way to construct the ESO solution. The present process takes place from the largest scale toward the smallest one, with gentler transitions between each level. The different scales are successively evolved during the process and three of them are distinctly identifiable:

1. From 0% to 7.23%:  $k_p$  material surrounds the whole finite-size volume and split it into two parts

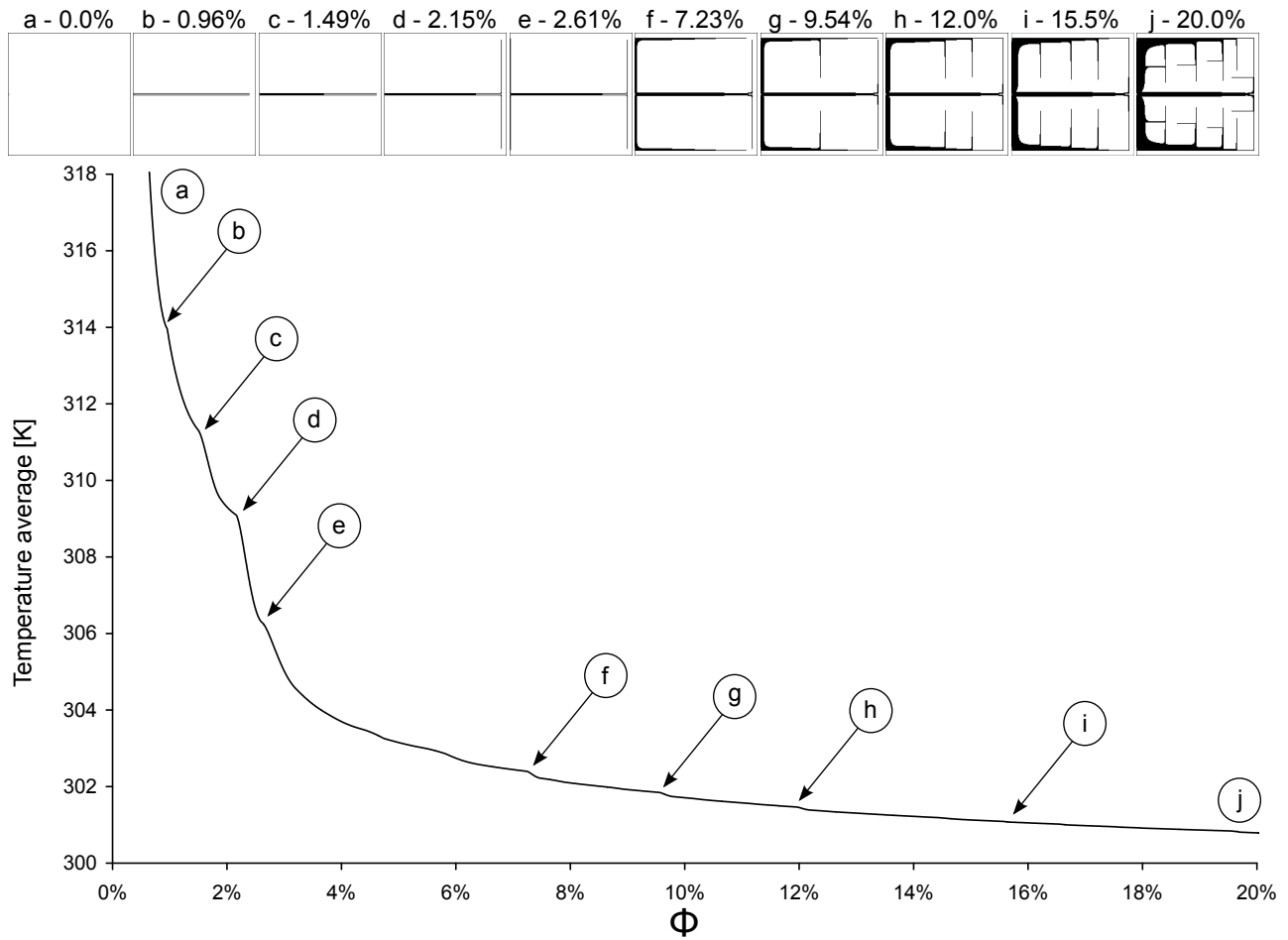


**FIGURE 5.** History of construction highlighting the outstanding points with their respective geometry and porosity

from the symmetry axis. This step can be seen as the first scale, *i.e.* the largest one.

2. From 7.23% to 15.5%: from the first level structure, six main dendrites (three for each side) are spread through the  $k_0$  material, following the heat sink direction. This additional high conductivity material never intersects itself and builds the second scale.
3. From 15.5% to 20.0%: from the two first scales, smaller extra dendrites are built towards virgin territories. They mainly turn back towards the heat sink and intersections may occur with second level structure.

Fig. 5 also emphasizes several discontinuities at regular intervals, which becomes manifest if the derivative function is established. The  $k_p$  geometry at each discontinuity is pictured at the top of Fig. 5, underlining that each of them matches a key step in the orientation of the extension process. For the first scale between

(a) and (f), each discontinuity is linked with a change of direction during the surrounding of  $k_0$  material. The three discontinuities of the second scale, included between (f) and (i), correspond to the establishing of its three dendrites. A similar behaviour is observable for the third construct and the growth of its own dendrites. An interesting phenomenon occurs before the construction of a new dendrite and after the establishing of the previous one: the previous scales are consolidated with additional  $k_p$  material. In other words, the creation of a new dendrite draining additional flux is always followed with a strengthening of the main structure.

Another point brought by Fig. 5 is relative to the effectiveness of  $k_p$  material addition, which becomes less efficient during the construction. For instance, between (i) and (j) almost 25% of the allocated material has been used to decrease the objective function value of only a few tenths of percent. Similar comments about constructal approach applied to this problem have been

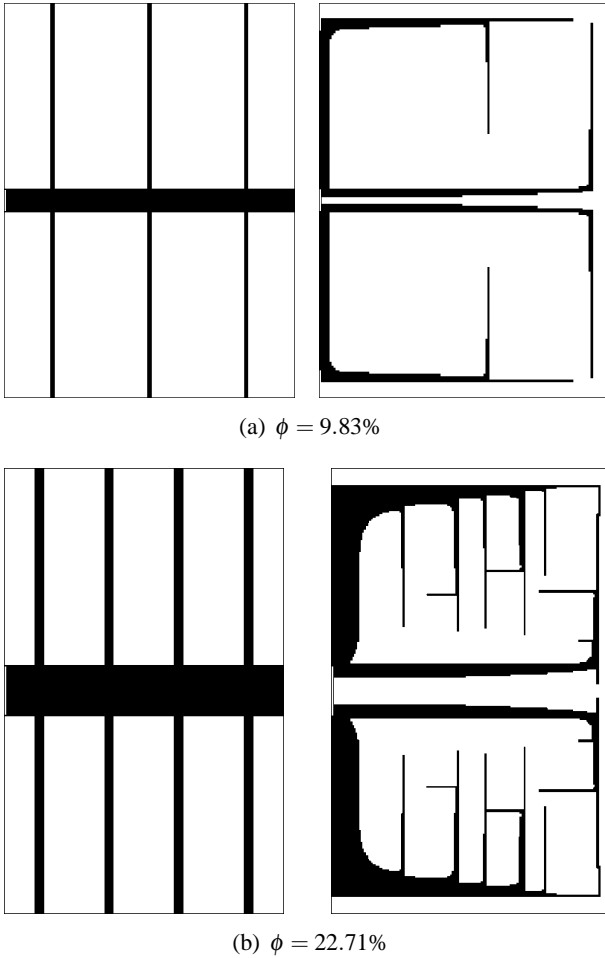


**FIGURE 6.** Qualitative comparison between two constructal geometries [10] and their associated ESO solution

formulated in [3].

### COMPARISON BETWEEN ESO AND CONSTRUCTAL METHODS

A comparison between a constructal geometry coming from [10] and the ESO approach introduced as so far is led, since both methods have been developed under the same physical assumptions. The selection of the constructal geometry is based on [2] which underlines that the cooling efficiency is not enhanced beyond the first constructal level. Consequently, two first order constructs are built with respectively six and eight elemental volumes ( $n_1$ ). Using the correlations given by [10] and for  $\hat{k} = 400$ , the porosity of these structures is respectively  $\phi_1 = 9.8\%$  and  $22.7\%$ .

The comparison made with constructal geometries implies structures with the same external dimensions,

$n_1$	$\phi$ %	$R_1$		$A_1$	
		Const.	ESO	Const.	ESO
6	9.8	0.0301	0.0229	0.0173	0.0159
8	22.7	0.0115	0.00955	0.00641	0.00603

**TABLE 1.** Quantitative comparison between two constructal geometries [10] and their associated ESO solution

length of heat sink and porosity. The thermal performance of each structure is calculated with the commercial finite volume code FLUENT<sup>®</sup>, using exactly the same mesh methods and numerical solver, which are fully detailed in [3]. They are evaluated with the same criterion coming from constructal and ESO approach. On one hand, the adimensionalized thermal resistance is minimized and defined as [1]:

$$R_1 = \frac{T(L, H/2) - T_s}{q''' LH/k_0} \quad (4)$$

On the other hand, ESO approach uses average temperature, which is a field criteria, to design the structure. It is not so far from constructal philosophy which aims “to connect a finite area ( $A$ ) to a single point ( $M$ )” with high conductivity material [1]. Thereafter, mathematical assumptions lead to minimize the warmest point, but the fact remains that it initially aimed to access to every point of the finite-size volume, *i.e.* reduce each local thermal resistance. The adimensionalized average criterion is noted:

$$A_1 = \frac{\bar{T} - T_s}{q''' LH/k_0} \quad (5)$$

Both geometries are displayed in Fig 6, showing better performances with ESO methods, as underlined in Table 1. In ESO configurations, the warmest temperature is located in the center of  $k_0$  material surrounded by  $k_p$ , and not anymore in the upper right-hand side corner, as in constructal structures. The better thermal performances of ESO structures can be evaluated with a different perspective: less high conductivity material is required to reach the same efficiency than the one of constructal design. For instance, the porosity of ESO structure can be reduced of 9.2% for  $n_1 = 6$ . Qualitatively, Fig. 4 and Fig. 6 show similarities with geometrical constructal enhancements studied by several authors. At first, the approach by scales used in constructal and fractal theories is also identifiable for ESO

structures. Secondly, three local geometry adaptations existing in constructal theory are brought through ESO:

1. The spacing at tips has been introduced by Almgöbel and Bejan in 1999 [11]: their study rests on giving the design more degrees of freedom and allowing the tip of high conductivity slab to be surrounded by  $k_p$  material. This feature also exists in ESO method, particularly in Fig. 4, where no  $k_p$  material from the smallest scale hits the central high conductivity path.
2. The second enhancements brought to constructal theory is relative to non-uniformly distributed tree-shaped structure [12]. In other words, the elemental volumes making the whole finite-size volume have a varying width, allowing fitting their size to reach a better cooling. This characteristic is shown in Fig. 6 which displays a compactness of dendrites in the same area.
3. In 2007, constructal approach have been improved once again, involving a variable cross section of conducting path [13]. This last design attribute is visible on each figure implying ESO geometries. If the heat sink is considered as a starting point, the cross section of the path becomes thinner when high conductivity material goes into the finite-size volume (Fig. 6(b)).

## CONCLUSION

Based on a switching principle of boundary elements, the ESO method builds a tree-shaped network through a step-by-step approach [9]. Comparing with meta-heuristic methods, such as GAs or SAs, this method takes advantage of its fully deterministic nature. Along this study, the classical ESO approach has been slightly modified from its classical formulation, especially regarding the degeneration of  $k_p$  material which has been reversed.

The iterative method of the implemented algorithm lies mainly on the continuity hypothesis of  $k_p$  material through the finite-size volume. The changes made on the structure are performed after a test loop which aims carrying out the sensitivity analysis in a direct way. The algorithm developed allows tackling global objective functions, instead of restricting their outreach to local objectives [9]. Such as defined in this study, the ESO by extension method can be easily parallelized to perform quickly the sensitivity analysis on the boundary

A quantitative comparison shows that the reached ESO geometries are more efficient than constructal designs in accordance with different thermal criterion. Even though the ESO structures show a more important  $k_p$  material accumulation around the heat sink, they present structural features which are closed to the ones developed in the latest modifications of constructal theory, as underlined in the last section.

## REFERENCES

- [1] Bejan, A., 1997. "Constructal-theory network of conducting paths for cooling a heat generating volume". *International Journal of Heat and Mass Transfer*, **40**(4), pp. 799 – 811.
- [2] Ghodoossi, L., 2004. "Conceptual study on constructal theory". *Energy Conversion and Management*, **45**(9-10), pp. 1379 – 1395.
- [3] Marck, G., Harion, J.-L., Nemer, M., Russeil, S., and Bougeard, D., 2011. "A new perspective of constructal networks cooling a finite-size volume generating heat". *Energy Conversion and Management*, **52**(2), pp. 1033–1046.
- [4] Xia, Z.-Z., Li, Z.-X., and Guo, Z.-Y., 2002. "Heat conduction optimization: high conductivity constructs based on the principle of biological evolution". In *Heat Transfer, P. of the Twelfth International Heat Transfer Conference*, ed., Elsevier SAS.
- [5] Cheng, X., Li, Z., and Guo, Z., 2003. "Constructs of highly effective heat transport paths by bionic optimization". *Science in China (serie E)*, **46**(3), pp. 296 – 302.
- [6] Boichot, R., Luo, L., and Fan, Y., 2009. "Tree-network structure generation for heat conduction by cellular automaton". *Energy Conversion and Management*, **50**(2), pp. 376 – 386.
- [7] Xu, X., Liang, X., and Ren, J., 2007. "Optimization of heat conduction using combinatorial optimization algorithms". *International Journal of Heat and Mass Transfer*, **50**(9-10), pp. 1675 – 1682.
- [8] Li, Q., Steven, G. P., Querin, O. M., and Xie, Y. M., 1999. "Shape and topology design for heat conduction by evolutionary structural optimization". *International Journal of Heat and Mass Transfer*, **42**(17), pp. 3361 – 3371.
- [9] Li, Q., Steven, G. P., Xie, Y., and Querin, O. M., 2004. "Evolutionary topology optimization for temperature reduction of heat conducting fields". *International Journal of Heat and Mass Transfer*, **47**(23), pp. 5071 – 5083.
- [10] Kuddusi, L., and Denton, J. C., 2007. "Analytical solution for heat conduction problem in composite slab and its implementation in constructal solution for cooling of electronics". *Energy Conversion and Management*, **48**(4), pp. 1089 – 1105.
- [11] Almgöbel, M., and Bejan, A., 1999. "Conduction trees with spacings at the tips". *International Journal of Heat and Mass Transfer*, **42**(20), pp. 3739 – 3756.
- [12] Almgöbel, M., and Bejan, A., 2001. "Constructal optimization of nonuniformly distributed tree-shaped flow structures for conduction". *International Journal of Heat and Mass Transfer*, **44**(22), pp. 4185 – 4194.
- [13] Zhou, S., Chen, L., and Sun, F., 2007. "Optimization of constructal volume-point conduction with variable cross section conducting path". *Energy Conversion and Management*, **48**(1), pp. 106 – 111.